NEURO-CLASSIFICATION OF MULTI-TYPE LANDSAT THEMATIC MAPPER DATA

Xin Zhuang and Bernard A. Engel
Agricultural Engineering Department
and
Laboratory for Applications of Remote Sensing

R. Norberto Fernández and Chris J. Johannsen
Laboratory for Applications of Remote Sensing
Purdue University
West Lafayette, IN 47907

ABSTRACT

Neural networks have been successful in image classification and have shown potential for classifying remotely sensed data. This paper presents classifications of multi-type Landsat Thematic Mapper (TM) data using neural networks. The Landsat TM image for March 23, 1987 with accompanying ground observation data for a study area in Miami County, Indiana, U.S.A. was utilized to assess recognization of crop residues. Principal components and spectral ratio transformations were performed on the TM data. In addition, a layer of the geographic information system (GIS) for the study site was incorporated to generate GIS-enhanced TM data. This paper discusses (1) the performance of neuro-classification on each type of data, (2) how neural networks recognized each type of data as a new image and (3) comparisons of the results for each type of data obtained using neural networks, maximum likelihood and minimum distance classifiers.

INTRODUCTION

Artificial intelligent networks have been applied to image classification of a variety of remotely sensed data, including Landsat Multispectral Scanner (MSS) data (Benediktsson, *et al.*, 1990a), Thematic Mapper (TM) data (Hepner *et al.*, 1990 and Civco, 1991), Advanced Very High Resolution Radiometer (AVHRR) and Scanning Multispectral Microwave Radiometer (SMMR) data (Key *et al.*, 1989), synthetic aperture radar (SAR) data (Decatur, 1989), and very high dimensional data - more than 20 channels (Benediktsson *et al.*, 1990b). Most of them showed promising results compared to traditional classification methods using maximum likelihood and minimum distance and great potential. A major advantage of neural network classifiers is that an assumption about distribution of data is not needed. The neural network classifier is able to extract automatically the features of data used in training and to apply them to the classification of data for the entire image.

For an early Spring image, classification of crop residues would involve much confusion between crop residues and bare soil because of low solar angle and high soil moisture. Crop residue is the portion of a crop that remains in the field after harvest. It is an important natural resource — not a waste as some have termed it (Oschwald,

1978). The residue left in a field can reduce soil erosion and protect water quality. Therefore, the image data have to be enhanced before classification in order to select representative training samples. Incorporating some GIS layer information may also help classification of crop residues.

The objective of this study was to investigate performance of neuro-classification of multi-type of remotely sensed data. The data include Landsat TM data, the transformed Landsat TM data produced by using principal components and spectral ratioing and the GIS-enhanced data generated by using digital land ownership information. Comparisons of classification results by applying neural networks, minimum distance and maximum likelihood were also made.

NEURO-CLASSIFICATION REVIEW

Benediktsson *et al.* (1990a) compared the classification performances of neural networks and statistical methods on a Landsat MSS data set augmented with topographic information including elevation, slope and aspect. The neural networks used were configured as a three-layer back-propagation network with full interconnections between adjacent layers; the delta rule and the generalized delta rule were utilized. Results showed that the neural network approach was more accurate than the statistical methods in terms of classification accuracy of training data. In another study, Benediktsson *et al.* (1990b) classified simulated high resolution imaging spectrometer data using several neural networks and statistical methods. They used twenty-, forty- and sixty-band data sets. The statistical approaches obtained the better results in all cases because the simulated data used in the study were generated to have a Gaussain distribution.

Hepner *et al.* (1990) concluded that the neural network classifier with a back-propagation algorithm, when using a minimal training data set, performed well for all areas including those for which the conventional supervised maximum likelihood method did not. In their study, a four-band Landsat TM data set (bands 1, 2, 3 and 4) associated with four broad land cover classes was classified using a three-layer back-propagation network. Civco (1991) classified a Landsat TM imagery for fifteen different land cover classes using three- and four-layer (one and two hidden layers, respectively) back-propagation networks. The accuracy results from the lumped seven-class land cover data showed that the maximum likelihood classifier performed generally better than the neural networks.

A merged image of AVHRR and SMMR data for an Arctic area was classified by Key *et al.* (1989) using traditional and neural network classifiers. The network was three-layered. They found that the neural network classifier had greater flexibility than the maximum likelihood classifier for classifying indistinct classes, such as those containing pixels with spectral values significantly different from the pixels in the training areas. In a classification of SAR data with three classes, Decatur (1989) concluded that the neural network classifier presented better results than the Bayesian classifier when accurate assumptions about probability density functions could not be make and *a priori* probability could not be given. However, it should be pointed out that in his study only three distinctive land-cover types were used and that SAR data generally do not have a Gaussian distribution.

DATA

Site Description

A study area of approximately 10.36 km^2 was comprised of sections 3, 4, 9 and 10 located in T28N, R5E of Richland township, Miami County, Indiana. Land cover for these sections included corn residues, soybean residues, grassland, forests, roads, an abandoned railroad, farmsteads and the Eel River. Portions of the area are owned by 58 farmers. This area is representative of much of northern Indiana and other states of the midwestern U.S.

Landsat TM Data

A Landsat TM scene acquired 23 March 1987 was used in this project, along with accompanying ground observation data for section 9. Aerial photographs from 1987 for this study area were available. The U.S. Geological Survey 1:24,000 topographic map of the Roann, Indiana Quadrangle was used as a reference. Principal components and spectral ratioing transformations were performed on the TM data, and two transformed image data sets were produced. The corresponding ownership map was digitized using ERDAS (ERDAS, 1988), and an ownership boundary data layer registered to 30-meter TM data was generated.

Transformed Data

Principal components transformation was performed to enhance images for maximum contrast and to make images visually more interpretable. Although principal components transformation does not enhance separability for the traditional classification techniques (Richards, 1987), it was employed to investigate whether neural network classification techniques perform differently after such a transformation. Moreover, considering the awareness of the lower-order principal components (Mather, 1987), all seven components were included.

An enhanced image can be generated from the division of digital values in one spectral band by the corresponding values in another band. These ratios clearly portray the variations in the slopes of the spectral reflectance curves between the two bands involved. In this study the difference between crop residues and bare soil was greater in band 5 than in band 6 for March data. Therefore, spectral ratioing was applied for crop residue discrimination. The function of this computing procedure was a modification of *Normalized Difference Vegetation Index (NDVI)* (Mather, 1987) and was defined as:

$$\frac{X_5 - X_7}{X_5 + X_7} \times 255$$

The symbols X_5 and X_7 refer to values of Landsat TM bands 5 and 7, respectively. The transformed data were used to replace the thermal infrared band of data (band 6) of the original TM data.

GIS-Enhanced Data

The GIS data layer used in this study was the ownership map associated with the four sections studied. The map was added as an eighth band to the Landsat TM image data called GIS-enhanced TM data. The reason for choosing the ownership

layer were that the ownership boundaries matched field boundaries. Each enclosed region represented one owner and was coded with a digital number (*i.e.*, each was numerically uniform), and thus the classification results may be improved because of the unique digital number inside each ownership polygon. It is assumed that each owner would apply the same residue management techniques to each field with an ownership unit.

METHODS

Neural Networks

The neural network used in this study, as shown in Figure 1, was configured as a three-layer back-propagation network, including input, hidden and output layers, with full interconnections between adjacent layers. The input layer was composed of an Nx8 array of binary-coded units corresponding to N bands (N = 7 or 8 in this study) of the 8-bit Landsat TM data. Thirty-five units were assigned to the hidden layer, and seven thermometer-coded units in the output layer referred to seven land cover classes. With thermometer coding, for example, class 4 of the seven categories would be represented as 1 in four most-significant bits and 0 in the remaining three bits (*e.g.* 4 = 1 1 1 1 0 0 0). For the training of a neural network, the TM data were fed to the input layer and propagated through the hidden layer to the output layer, and then the differences between the computed outputs and the desired outputs were calculated and fed backward to adjust network parameters. This process continued until the training arrived at a desired error. Additional details of the network are given in Zhuang (1990).

The neural networks simulator used was NASA NETS (Baffes, 1989), which runs on a variety of machines including workstations and PCs. The simulator provides a flexible system for manipulating a variety of neural network configurations using the generalized delta back-propagation learning algorithm. The NETS software used for image classification was run on SUN SPARC workstations. Interface routines were developed to make NETS suitable for image classification (Zhuang, 1990).

Classification

The neural network (NN), minimum distance (L1) and maximum likelihood (ML) classifiers were applied to the Landsat TM data. The minimum distance classifier used in this study classified an unknown pixel by computing the L1 distance (Richards, 1986) between the value of the unknown pixel and each of the information class means, and then assigned the unknown pixel to the "closest" information class. Under the assumption of normality, the maximum likelihood classifier categorized a given pixel by computing the statistical probability of the pixel being a member of particular information class. The neural network classified an unknown pixel by applying the knowledge learned from a training data set to the pixel. For the study area, training fields were selected for seven different land cover classes based on the corresponding ground observation data and spectral features. The classes were: *corn/50%* (corn residue, 50% ground cover), *corn/83%* (corn residue, 83% ground cover), *forest*, *pasture/grass*, *river*, *soybeans/64%* (soybean residue, 64% ground cover) and *bare soil*. The training data for class *river* were obtained by unsupervised classification (clustering) of the portion of the images containing the river.

For the principal components transformed data set, a classification using a neural network was performed. The neural network classifier recognized the transformed data, which was uncorrelated after transformation in the multispectral vector space, as a new image and determined the features from the transformed training data. For the spectral ratioing transformed data set, the classification using maximum likelihood and minimum distance were executed in addition to a neuro-classification. For the GIS-enhanced data set, it was not possible to complete the maximum likelihood classification because the second-order statistics of the land ownership layer were not meaningful. The neural network classifier was utilized because it need not address the second order statistic, *covariance*. Since the minimum distance classifier considers only the first order statistic, *mean*, it was possible to use this classifier for classification of the GIS-enhanced data set.

RESULTS AND DISCUSSION

Tables 1 through 9 show accuracy data obtained by using minimum distance (L1), maximum likelihood (ML) and neural networks (NN) for the Landsat TM data set, principal components (PC) and spectral ratioing (SR) transformed data sets and the GIS-enhanced TM data set. Separate testing data were selected from each multi-type of image. As listed in Tables 1, 2 and 3, L1, ML and NN achieve for the entire testing data overall classification accuracies of 73%, 96% and 91%, respectively. Table 4 presents the results for the PC transformed data set obtained using a neural network. The accuracy was 90%. Tables 5, 6 and 7 illustrate the results with 84%, 96% and 91% accuracies for the SR transformed data set obtained using L1, ML and NN. The testing results with 71% and 95% accuracies for the GIS-enhanced TM data, which were classified by using L1 and NN, are listed in Tables 8 and 9.

The neural network classifiers used in this study not only presented promising classification results for the multi-type Landsat TM data sets but also did recognize each type of image data as a new data set. The accuracies of entire testing data set for four neural network classifications are all more than ninety percent, as shown in Tables 3, 4, 7 and 9. Therefore, it can be concluded that NN could classify a variety of different format images and provided great accuracy to each of them.

Compared with the performances of minimum distance and maximum likelihood, the neural network used for each individual type of image in this study performed consistently well. For the Landsat TM data and the SR transformed data, the NN presented 91% accuracy though it was five percent less than the accuracy obtained by ML. In addition to 90% accuracy for the PC transformed testing data set, NN achieved higher accuracies for crop residue classes in which we were interested than those of the Landsat TM data. For the GIS-enhanced TM data, ML could not work because of the reason described before. However, NN performed 95% accuracy for the entire testing data set and more than 88% for each individual class. Moreover, it can be noticed that the performance of neural network classification was improved when incorporating the digital land ownership data, compared to the performances exhibited from other three type of data sets (Landsat TM, PC and SR). Of all nine classifications done in this study, the neural network classifiers presented less confusion between the bare soil class and any other class.

The map results for each type of image are collectively depicted in Figure 2. These map results show clearly the comparisons among classifications of each type of images and the four neural network classifications. Confusions for each image reflected in its confusion matrix listed in Tables 1 through 9 are also illustrated in Figure 2. The improvement with neural network classification on the GIS-enhanced TM data mentioned above is clearly shown in the corresponding map print-out.

Maximum (Max) and *Root Mean Square* (RMS) errors are two parameters to monitor and adjust the training for neural networks in this study. A Max error was the maximum among the differences between each actual output and desired output in the output layer, whereas a RMS error referred to the root mean square of the differences. The training performance for each type of data set is illustrated in Figure 3 and 4. Each training stopped at a Max error of 10%. As shown in Figure 3 and 4, it took more than two times as long to train the transformed data sets than the Landsat TM data set, while the training for the Landsat TM data was slightly different from that for the GIS-enhanced TM data. In terms of the training convergency, it can be seen that the neural network trainings for the PC and SR transformed data were less smooth than that for the Landsat TM data. Moreover, the training of the neural network used to classify the GIS-enhanced TM data converged faster than other three trainings.

CONCLUSION

Neural networks can be used to classify multi-type images and provided very promising results. A neural classifier recognized each of multi-type images as a new data set no matter whether it was transformed or generated. By incorporating the digital land ownership data, the classification for crop residues using a neural network achieved better accuracy than those from other types of data sets. The neural network classifiers in this study presented less confusion between the bare soil class and any other class.

ACKNOWLEDGEMENTS

The authors wish to acknowledge with the gratitude the support of this research by NASA (Grant# NAGW-1472). We also would like to thank Dr. M. Baumgardner, Dr. P. Swain and Dr. D. Jones for their evaluation of the analysis and results of this research, Mr. Jack Hart for his collection of ground observation data, Dr. Fabián Lozano-García for his assistance in providing satellite image data, Dr. David Landgrebe ipfor his permission to access the Image Processing Laboratory in the School of Electrical Engineering, Purdue University, and Mr. Larry Biehl for his assistance with the *MultiSpec* image processing system.

REFERENCES

1. Baffes, P.T., 1989. *Nets User's Manual. Version 2.0.* AIS at NASA/JSC, Athens, GA.

2. Benediktsson J.A., P.H. Swain, and O.K. Ersoy, 1990a. Neural network approaches versus statistical methods in classification of multisource remote sensing data. *IEEE Trans. Geoscience and Remote Sensing,* GE-28(4): 540-552.

3. ——, 1990b. Classification of very high dimensional data using neural networks. *IGARSS' 90*, Vol. 2, pp. 1269-1272.

4. Civco, D.L., 1991. Landsat TM image classification with an artificial neural network. *Proceedings of the 1991 Annual ASPRS-ACSM Convention*, Baltimore, MD. Vol 3, pp 67-77.

5. Decatur, S.E., 1989. Application of neural networks to terrain classification. *Proceedings of the 1989 International Joint Conference on Neural Networks*, Washington, D.C., Vol. 1, pp. 283-288.

6. ERDAS, Inc., 1988. *ERDAS User's Guide. Version 7.3.*

7. Hepner, G.F., T. Logan, N. Ritter, and N. Bryant, 1990. Artificial neural network classification using a minimal training set: comparison to conventional supervised classification. *Photogrammetric Engineering and Remote Sensing*, 56(4): 496-473.

8. Key, J., J.A. Maslanik, and A.J. Schweiger, 1989. Classification of merged AVHRR and SMMR Arctic data with neural networks. *Photogrammetric Engineering and Remote Sensing*, 55(9): 1331-1338.

9. Mather, P.M., 1987. *Computer Processing of Remotely-Sensed Images : An Introduction*, John Wiley & Sons, Inc., pp. 179-241.

10. Oschwald, W.R., M. Stelly, D.M. Kral, and J.H. Nauseef, 1978. *Crop Residue Management Systems.* ASA Special, Vol. 31, pp. 1-48.

11. Richards, J.A., 1986. *Remote Sensing Digital Image Analysis : An Introduction.* Springer-Verlag, Berlin, West Germany, 281p.

12. Zhuang, X., 1990. *Determining Crop Residue Type and Class Using Satellite Acquired Data*, M.S.E. Thesis, Department of Agricultural Engineering, Purdue University, West Lafayette, IN. 129p.

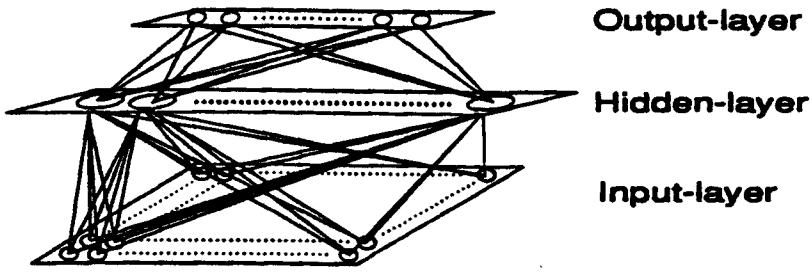

Figure 1. The back-propagation neural network structure.

Table 1. Confusion matrix for the Landsat TM testing data classified using minimum distance (L1) algorithm.

TM classes	Percent correct	Ground observation classes C/50%	C/83%	F	P	S/64%	Total
corn/50%	84%	608	2	0	22	4	634
corn/83%	89%	16	64	2	4	6	92
forest	69%	0	2	95	4	0	101
pasture	59%	0	0	0	253	5	258
river	—	0	0	48	0	0	48
soybeans/64%	75%	88	7	0	134	62	291
bare soil	—	15	0	0	32	6	53
No. of ground obs. pixels	73%	725	75	145	449	83	1477

Table 2. Confusion matrix for the Landsat TM testing data classified using maximum likelihood (ML) algorithm.

TM classes	Percent correct	Ground observation classes C/50%	C/83%	F	P	S/64%	Total
corn/50%	97%	705	4	0	0	0	709
corn/83%	97%	1	71	0	0	0	72
forest	100%	0	0	145	2	0	147
pasture	93%	2	0	0	418	5	425
river	—	0	0	0	1	0	1
soybeans/64%	89%	2	0	0	23	74	99
bare soil	—	15	0	0	5	4	24
No. of ground obs. pixels	98%	725	75	145	449	83	1477

Table 3. Confusion matrix for the Landsat TM testing data classified using neural network (NN) approach.

TM classes	Percent correct	Ground observation classes C/50%	C/83%	F	P	S/64%	Total
corn/50%	97%	706	17	1	9	1	734
corn/83%	77%	10	58	3	7	3	81
forest	94%	1	0	136	5	2	144
pasture	88%	8	0	4	395	18	425
river	—	0	0	1	3	1	5
soybeans/64%	65%	0	0	0	28	54	82
bare soil	—	0	0	0	2	4	6
No. of ground obs. pixels	91%	725	75	145	449	83	1477

Table 4. Confusion matrix for the PC transformed testing data classified using neural network (NN) approach.

TM classes	Percent correct	Ground observation classes C/50%	C/83%	F	P	S/64%	Total
corn/50%	98%	709	12	1	11	0	733
corn/83%	89%	4	69	0	2	1	70
forest	97%	2	0	141	21	5	169
pasture	81%	6	0	1	383	14	384
river	—	0	0	2	9	1	12
soybeans/64%	71%	2	0	0	37	59	98
bare soil	—	2	0	0	6	3	11
No. of ground obs. pixels	90%	725	75	145	449	83	1477

Table 5. Confusion matrix for the SR transformed testing data classified using minimum distance (L1) algorithm.

TM classes	Percent correct	Ground observation classes C/50%	C/83%	F	P	S/64%	Total
corn/50%	85%	615	3	0	0	3	621
corn/83%	96%	91	72	0	0	0	163
forest	86%	0	0	125	4	0	129
pasture	80%	0	0	0	360	7	367
river	—	0	0	20	0	0	20
soybeans/64%	83%	5	0	0	71	69	145
bare soil	—	14	0	0	14	4	32
No. of ground obs. pixels	84%	725	75	145	449	83	1477

Table 6. Confusion matrix for the SR transformed testing data classified using maximum likelihood (ML) algorithm.

TM classes	Percent correct	Ground observation classes C/50%	C/83%	F	P	S/64%	Total
corn/50%	97%	701	4	0	0	0	705
corn/83%	97%	2	71	0	0	0	73
forest	100%	0	0	145	3	0	148
pasture	94%	3	0	0	421	3	427
river	—	5	0	0	0	0	5
soybeans/64%	92%	2	0	0	21	76	99
bare soil	—	12	0	0	4	4	20
No. of ground obs. pixels	98%	725	75	145	449	83	1477

Table 7. Confusion matrix for the SR transformed testing data classified using neural network (NN) approach.

TM classes	Percent correct	Ground observation classes C/50%	C/83%	F	P	S/64%	Total
corn/50%	94%	678	32	0	0	0	710
corn/83%	57%	13	43	0	3	0	59
forest	89%	1	0	129	7	0	137
pasture	92%	13	0	15	412	9	449
river	—	2	0	1	8	0	11
soybeans/64%	88%	18	0	0	15	73	106
bare soil	—	0	0	0	4	1	5
No. of ground obs. pixels	90%	725	75	145	449	83	1477

Table 8. Confusion matrix for the GIS-enhanced TM testing data classified using minimum distance (L1) algorithm.

TM classes	Percent correct	Ground observation classes C/50%	C/83%	F	P	S/64%	Total
corn/50%	81%	589	2	0	2	4	597
corn/83%	88%	14	66	2	7	1	90
forest	92%	0	2	133	2	0	137
pasture	39%	4	1	0	176	0	181
river	—	0	0	10	0	0	10
soybeans/64%	94%	96	4	0	157	78	345
bare soil	—	22	0	0	95	0	117
No. of ground obs. pixels	91%	725	75	145	449	83	1477

Table 9. Confusion matrix for the GIS-enhanced TM testing data classified using neural network (NN) approach.

TM classes	Percent correct	Ground observation classes C/50%	C/83%	F	P	S/64%	Total
corn/50%	100%	723	9	1	17	1	751
corn/83%	88%	1	66	0	6	0	73
forest	99%	1	0	144	5	1	151
pasture	89%	0	0	0	401	5	406
river	—	0	0	0	1	1	2
soybeans/64%	90%	0	0	0	12	75	87
bare soil	—	0	0	0	7	0	7
No. of ground obs. pixels	95%	725	75	145	449	83	1477

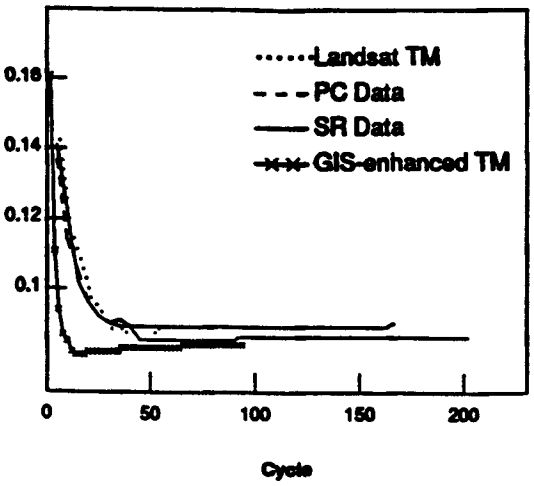

Figure 3. Root Mean Square errors for all neural trainings.

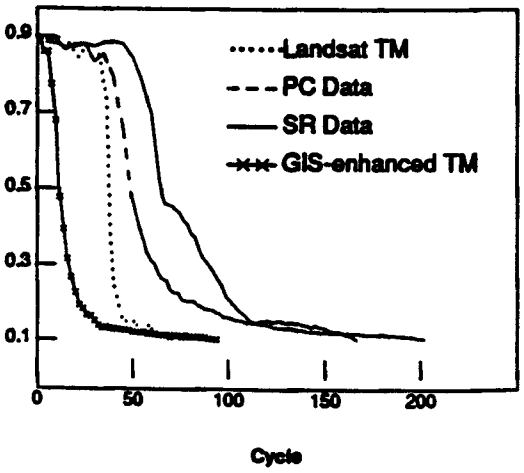

Figure 4. Maximum errors for all neural trainings.

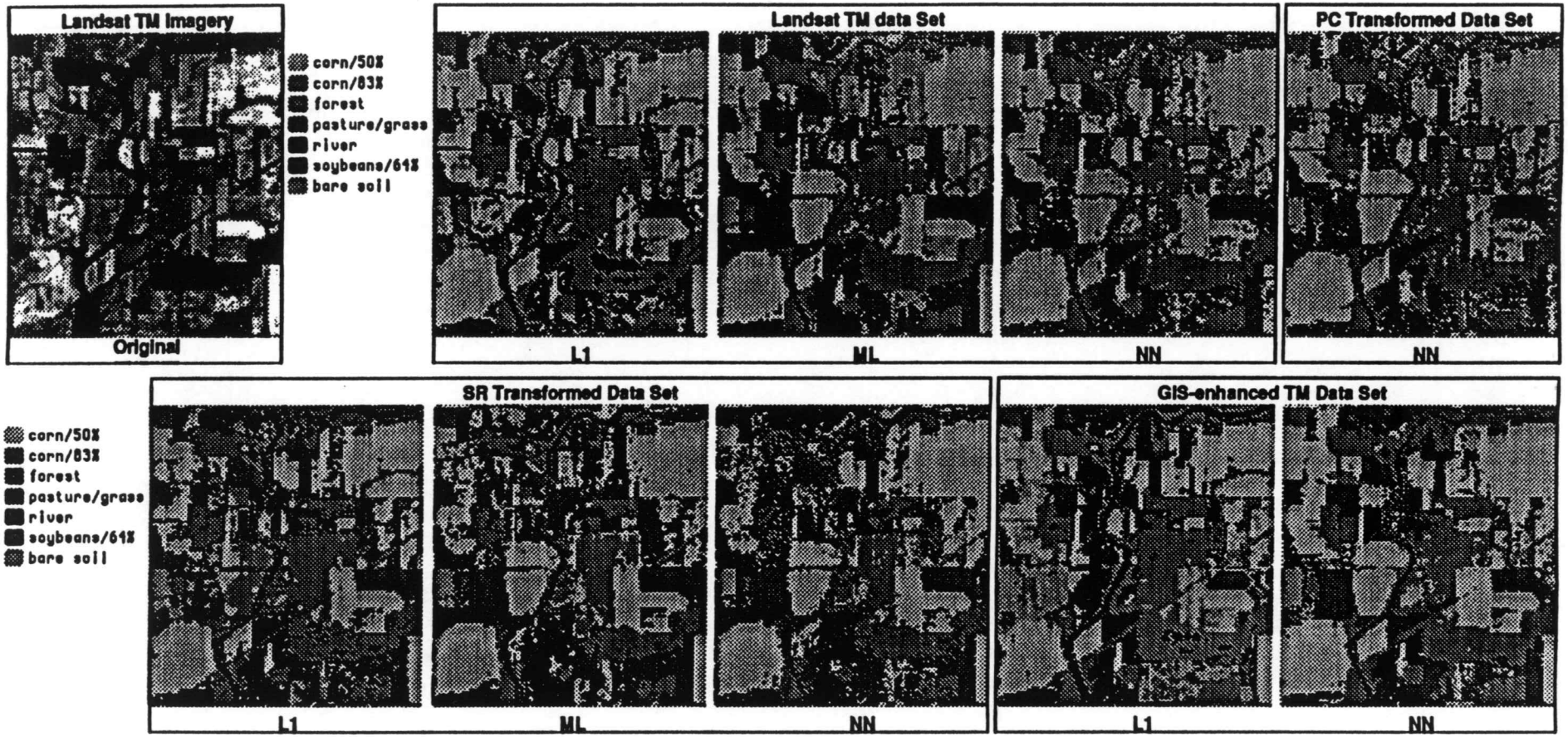

Figure 2. Landsat imagery and the classification results of multi-type images.
(Legends are associated with the classification results.)